Published in final edited form as:
Chemistry. 2010 September 10; 16(34): 10418–10423. doi:10.1002/chem.201000607.

Conformational Structure and Energetics of 2-Methylphenyl(2′-methoxyphenyl)iodonium Chloride: Evidence for Solution Clusters

Yong-Sok Lee[a], **Milan Hodošček**[b], **Joong-Hyun Chun**[c], and **Victor W. Pike**[c]

Yong-Sok Lee: leeys@mail.nih.gov

[a] Center for Molecular Modeling, Division of Computational Bioscience, Center for Information Technology, National Institutes of Health, Department of Health and Human Services, Building 12A, Room 2049, Bethesda, MD 20892, USA, Fax: (+1) 301 402 2867

[b] National Heart, Lung and Blood Institute, National Institutes of Health, Department of Health and Human Services, Bethesda, MD 20892, USA, & National Institute of Chemistry, Ljubljana, Slovenia

[c] Molecular Imaging Branch, National Institute of Mental Health, National Institutes of Health, Department of Health and Human Services, Room B3 C346A, Building 10, 10 Center Drive, Bethesda, MD 20892, USA

Abstract

Diaryliodonium salts allow the efficient incorporation of cyclotron-produced [^{18}F]fluoride ion into both electron-rich and electron-deficient arenes to provide potential radiotracers for molecular imaging *in vivo* with positron emission tomography (PET). This process ($ArI^{+}Ar' + {}^{18}F^{-} \rightarrow Ar^{18}F + Ar'I$) is still not well understood mechanistically. In order to better understand this and similar reactions, it would be valuable to understand the structures of diaryliodonium salts in organic media where the reactions are typically conducted. In this endeavor, the X-ray structure of a representative iodonium salt, 2-methylphenyl(2′-methoxyphenyl)-iodonium chloride (**1**) was determined. Our X-ray study showed **1** to have the conformational **M-P** dimer as the unit cell with hypervalent iodine as the stereogenic center in each conformer. With the *ab initio* replica path method, we constructed the inversion path between the two enantiomers of **1**, thereby revealing two additional pairs of enantiomers that are likely to undergo fast interconversion in solution. Also, LC-MS of **1** showed the presence of dimeric and tetrameric anion-bridged clusters in weakly organic (MeCN) solution. This observation is consistent with the energetics of **1**, both as monomeric and dimeric forms in MeCN, calculated at the level of B3LYP/DGDZVP. These evidences of the existence of solution dimeric and higher order clusters of **1** are relevant to achieving a deeper general understanding of the mechanism and outcome of reactions of diaryliodonium salts in organic media with nucleophiles, such as [^{18}F]fluoride ion.

Keywords

iodonium salt; stereogenic iodine; inversion path; dimer; energetic; clusters

Correspondence to: Yong-Sok Lee, leeys@mail.nih.gov.

Supporting information for this article is available on the WWW under http://www.chemeurj.org/ or from the author.

Introduction

Diaryliodonium salts (ArI^+ArX^-) widely serve as useful reagents for arylation and oxidation reactions.[1] They are also becoming very useful substrates for the preparation of fluorine-18 ($t_{1/2}$ = 109.7 min) labeled fluoroarenes as potential radiotracers for biomedical imaging with positron emission tomography (PET).[2] In view of these increasing synthetic applications, a detailed understanding of the structure of diaryliodonium salts in organic solution is desirable to assist in understanding reaction mechanisms and outcomes.

Previous studies have shown that diaryliodonium salts are in general fully dissociated in aqueous or polar media[3] but have also suggested that they may exist as ion pairs or dimeric structures in less polar organic solvents.[3,4] Solid-state structures determined with X-ray crystallography often prove diaryliodonium salts to be anion-bridged dimers held together by iodine-halogen bonds.[5] However, correspondence between solid-state and solution structure has not been elucidated previously. Here we present X-ray crystallography data on an example of an unsymmetrical diaryliodonium salt, 2-methylphenyl(2′-methoxyphenyl)iodonium chloride (**1**). Interestingly, these data unveiled hypervalent iodine as a previously unrecognized stereogenic center within a dimeric structure composed of conformational **M** and **P** enantiomers (Figure 1). An immediate consequence of the stereogenic iodine is the possible racemization of **1** in solution. In the present work, this racemization process was investigated with quantum chemistry at the level of B3LYP/DGDZVP. For this purpose, we utilized the *ab initio* replica path (RPATH) method[6,7] to construct the inversion path for the conformers **M** and **P** of **1**. This method readily identifies the transition state (TS) of a chemical reaction or conformational change of interest without prior knowledge of the TS geometry, as exemplified in our previous study of the inversion of 1,4-benzodiazepines.[7] We also found mass spectrometric evidence for solution clusters of **1**, and we therefore also carried out quantum chemical calculations to probe for the existence of dimeric **1** in MeCN, choosing the latter as a representative organic solvent.

Results and Discussion

X-Ray Structure and Interconversion of Conformational Enantiomers of 1

Our X-ray study found **1** to have the **M**–**P** dimer as the unit cell in a centrosymmetric crystal (Figure 2). In particular, the central iodine atoms of **M** and **P** are located above (7.6°) and below (−7.6°) the plane of C1–C8–Cl, respectively, as measured by their improper dihedral angles of I–C1–C8–Cl, and therefore show that the hypervalent iodine of **1** is stereogenic. A similar observation has been made for the sulfur of phenyl *p*-tolyl sulfoxide, which is known to racemize by pyramidal inversion.[8] Aside from the presence of a stereogenic iodine atom, the structure of **1** resembles those of Ph_2I–Z (Z = Cl, Br or I)[5] in that **1** forms a bridged dimer whose iodine coordination is square planar. One difference, however, is that the methoxy and methyl substituents render the chloride-bridge in **1** longer and more asymmetric (I–Cl = 3.101, 3.028 Å) than in Ph_2I–Cl (I–Cl = 3.065, 3.105 Å). The I–Cl bonds in **1** are primarily ionic since their lengths are about 0.64 Å longer than in solid $PhICl_2$ (2.46 Å).[9] It is this ionicity that allows the secondary bonds[10] to arise, so enabling the crystallization of **1** as the Cl-bridged dimer.

In our theoretical study, we first probed the racemization of **1** in the gas phase. The resulting potential energy surface (PES) obtained from the RPATH method is shown in Figure 3; the inset is a graphical representation of the 60 replicas that are superimposed with the best fit, using the six atoms (C1–C6) of the anisyl group of **M1** as the common docking point. The PES of Figure 3 gives three distinct conformers of **M** and **P** as well as two **TS**s that are best described by the rotation of two torsional angles, Cl-I-C8–C9 (φ_1) and C8–I–C1–C2 (φ_2), as shown in Figure 4. Note that the states shown in Figures 3 and 4 are approximate since

geometry at each replica was minimized with an added harmonic penalty function. The conformer **M2** is 2.2 kcal/mol more stable than **M1** due to less steric repulsion between the two aryl rings than in **M1**, achieved through an equatorial rotation of the tolyl group (φ_2) with respect to the anisyl group. Further rotation of the tolyl group gives rise to another conformer **M3** which is 1.2 kcal/mol more stable than **M1**. At $\mathbf{TS_1}$, the ionic I–Cl bond length (2.82 Å) is longer than in **M1** (2.75 Å) due to steric repulsion between the tolyl group and the Cl atom; this I–Cl bond weakening in $\mathbf{TS_1}$ is reflected in the 9.0 kcal/mol greater energy of $\mathbf{TS_1}$ relative to **M1**. Further rotation of φ_1 yields the conformer **P1**, a pseudo enantiomer of **M1**. Counter-clockwise rotation of the tolyl ring gives rise to **P2** and **P3**, the respective pseudo enantiomers of **M2** and **M3**, respectively. The energy of $\mathbf{TS_2}$ is 1.6 kcal/mol lower than that of $\mathbf{TS_1}$ due to the Cl atom being *anti* to the tolyl methyl group. The calculated energy barriers within the conformers of **M** or **P** are no higher than 2.6 kcal/mol, indicating that their interconversion at room temperature likely occurs on a picosecond timescale.

The approximate states in Figure 4 were further geometry-optimized with Gaussian 03 utilizing the polarized continuum model with the UAKS parameters set in MeCN.[11] Single imaginary frequencies for the vibrational-torsional motion of the tolyl group in the direction of **M3** or **P1** for $\mathbf{TS_1}$ ($-36.6\ cm^{-1}$) and of **P3** or **M1** for $\mathbf{TS_2}$ ($-39.4\ cm^{-1}$) were obtained, but none in any other conformers. In terms of energetics (Table 1), **M1** and **M3** are essentially isoenergetic while **M2** is only 0.7 kcal/mol more stable than either of these, due to the attenuated steric repulsion in MeCN. The inclusion of the solvent effect lengthened the ionic bond I–Cl in **M1** from 2.75 Å *in vacuo* to 2.87 Å and that in $\mathbf{TS_1}$ from 2.82 Å *in vacuo* to 3.08 Å. It also rendered $\mathbf{TS_1}$ and $\mathbf{TS_2}$ isoenergetic at 9.1 kcal/mol higher than **M1**, suggesting that the inversion of **1** occurs equally well via the enantiomeric $\mathbf{TS_1}$ or $\mathbf{TS_2}$ **(**not calculated), as in the case of benzodiazepines.[7] The energy barrier of 9.1 kcal/mol further suggests that the racemization at room temperature in MeCN occurs in the micro-second range, which is too fast to be investigated with NMR. In these circumstances, a theoretical approach, such as RPATH, seems the only viable way for studying the geometry of diaryliodonium salts and their energetics in organic solvents.

The superposition of the fully optimized structures onto the six atoms (C1–C6) of the anisyl group of **M1** as the common docking point gives a visual representation of each of the conformer pairs (Figure 5): the pairs **M1** and **P1**, **M2** and **P2** and **M3** and **P3** are enantiomers while $\mathbf{TS_1}$ and $\mathbf{TS_2}$ are not. These optimized structures further provide detailed information on the iodine inversion for each enantiomeric pair. Figure 6 shows the microscopic iodine inversion of **M1** to **P1** wherein the central iodine atoms of **M1** and **P1** are located above (2.0°) and below (−2.0°) the plane of C1–C8–Cl, respectively. These calculated improper dihedral angles are 5.6° smaller than those in the X-ray structure of **1**. On the **M1**–$\mathbf{TS_1}$–**P1** path, the iodine of **M1** first moves downwards with respect to the plane of C1–C8–Cl until the **M3** state is reached; the iodine then moves upwards to reach $\mathbf{TS_1}$, and downwards again to complete the inversion. The **P1**–$\mathbf{TS_2}$–**M1** path shows an opposite movement of the iodine atom, but this is not symmetric to the **M1**–$\mathbf{TS_1}$–**P1** path by inversion, because $\mathbf{TS_1}$ and $\mathbf{TS_2}$ are not enantiomers.

Evidence for Clusters of 1 from LC-MS, MS and Energetics Calculations

During the characterization of **1** in MeCN solution by LC-MS, we encountered the unexpected finding that reversed phase LC operated with water-methanol-acetic acid as mobile phase gave not a single sharp peak but a broad multi-peaked elution profile starting from elution near the solvent front (capacity factor, $k' \sim 1.0$) up to capacity factors of ~ 4 (see Supporting Information). MS of all material in this broad elution range gave a base peak at $m/z = 324.9$, corresponding to the monomeric cation of **1**, $[C_{14}H_{14}OI]^+$. Close scrutiny of these spectra also showed a set of low abundance ions beginning at *m/z* 684.3

and another set at 708.3. The former set, according to its isotope M and M+2 abundance ratio, contained one Cl atom, while the latter did not. The ion *m/z* 684.3 was deduced to be the Cl-bridged dimer $[(MeOC_6H_4IMeC_6H_4)_2Cl]^+$, uniquely generated from an unseen Cl-bridged tetrameric metastable ion with composition $[(MeOC_6H_4IMeC_6H_4)_4Cl_2 + H]^{2+}$. High resolution mass specteomtry confirmed the elemental composition of the detected dimeric ion, $[(MeOC_6H_4IMeC_6H_4)_2Cl]^+$ (see Supporting Information). Similarly, the ion at *m/z* = 708.3 was deduced to be an acetate-bridged dimer $[(MeOC_6H_4IMeC_6H_4)_2OAc]^+$ uniquely generated from an unseen acetate-bridged tetrameric metastable ion with composition $[(MeOC_6H_4IMeC_6H_4)_4OAc + H]^{2+}$ (Supporting Information). Incoporation of OAc^- into the latter must have occurred in the HPLC mobile phase. These obervations directly show the existence of stable dimeric and tetrameric clusters of **1** in even the weakly organic HPLC mobile phase. How might such clusters form?

As listed in Table 1, the six conformers of **1** are comparable in energy and thus all are likely to exist in MeCN at room temperature. These conformers could then form a dimer in organic solvent via the secondary bonding interaction[10] that was attributed to be the driving force for formation of the solid state dimeric structure. To investigate this possibility, quantum chemical calculations were performed on the three pairs of enantiomers; each dimer was constructed by manually putting their geometry optimized monomers together. Calculations were also performed on an **M1**–**M1** dimer for comparison. These calculations indicate that, in MeCN, the **M1**–**P1** heterodimer is more stable than **M1**–**M1** and **M3**–**P3** by 1.8 kcal/mol and 2.6 kcal/mol, respectively; the **M2**–**P2** dimer converged to the **M3**–**P3** dimer.

Figure 7 illustrates the energy-minimized structures of **M1**–**P1** and **M1**–**M1** in MeCN. The dimer **M1**–**P1** closely resembles the X-ray structure in Figure 2 as evidenced by both the root mean square deviation (rmsd) of 0.02 Å between the experimental and calculated bond distances and the less than 3° difference in bond angles (Table 3 in Supporting Information). The calculated I-Cl distances (3.09, 3.18 Å) in **M1**–**P1** are longer than that in monomeric **M1** or **P1** (2.87 Å) but are very comparable to those observed in the crystal structure (3.03, 3.10 Å). When **M1** approaches **P1** or vice versa, the Mulliken atomic charge on the iodine atom (+0.38) of **M1** forms a strong charge interaction with the negative charge on the chlorine atom (−0.70) of **P1** to form another ionic bond with a length of 3.18 Å. This charge interaction in turn polarizes the I–Cl bond of the monomers **M1** and **P1** as manifested by an increase in length from 2.87 to 3.09 Å. In line with this bond lengthening, the calculations showed a further polarization of the atomic charge on I (+ 0.44) and Cl (− 0.71) in the **M1**-**P1** dimer relative to those in the **M1** or **P1** monomer. Note that these atomic charges are comparable to other electrostatic potential-derived charges such as CHelpG.

With the zero point energy correction and thermal enthalpy contribution at 298.15 K, the ΔH for dimerization of **M1**–**P1** in MeCN, calculated by substracting the sum of the energy of each monomer from the energy of the **M1**–**P1** dimer, was − 9.0 kcal/mol. When the entropy contribution was included, ΔG for the dimerization became +2.8 kcal/mol. This is primarily due to the loss of the translational and rotational (TR) entropy of the two monomers upon dimerization, which is 91 $cal.mol^{-1}.K^{-1}$ or about 46*R* based on the ideal gas approximation. However, the TR entropy contribution of a solute to dimerization is known to be much lower in the liquid phase because of hindered movement. For example, the experimental TR entropy contribution to the dimerization of a protein in aqueous solution has been reported to be 5±4*R*, as opposed to 50*R* estimated from the ideal gas approximation.[12] Assuming the high end of the TR entropy (i.e., 9*R*), the ΔG for the dimerization of **M1** with **P1** was estimated to be −13.1 kcal/mol at 298.15 K. The basis set superposition error for **M1**–**P1** dimerization in the gas phase was only 1.4 kcal/mol and was thus unlikely to affect the calculated thermochemical stability of **M1**–**P1** in MeCN. These results, taken together, suggest that **1** predominantly exists as dimers in MeCN solution. While the thermochemical

stability of tetramers has not been considered due to lack of structural information, the LC-MS study suggests the existence of tetramers of **1** in solution. This might be driven by an increase in entropy of solvent molecules surrounding the more structurally ordered tetramers. Further experimental and theoretical efforts are needed to better explain the formation and stability of higher order clusters.

Besides being more stable than **M1**–**M1** and **M3**–**P3**, the **M1**–**P1** heterodimer has a negligible dipole moment (μ = 0.07 D). As a result, the dipole-dipole interaction among **M1**–**P1** dimers is minimal compared to **M1**–**M1** (μ = 0.82 D) or **M3**–**P3** (μ = 0.37 D). This may explain the formation of the **M1**–**P1** dimer as a unit cell in a centrosymmetric crystal. In the case of **M1**–**M1** or **M3**–**P3** dimer (not observed), the unit cell might well require doubling or even quadrupling in size to minimize the overall dipole moment of the crystal.

The favorable dimerization energy calculated here further indicates well-known reactions of diaryliodonium salts similar to **1** with nucleophiles in organic solvents may require the dissociation of dimers or possibly even tetramers. In the case of the increasingly useful radiofluorination reactions[2], such dissociation will likely be necessary to allow replacement of chloride ion with ^{18}F-fluoride ion, preceding attack of the bound fluoride ion onto an aryl carbon atom to give either of the two possible [^{18}F]fluorarene products.[13] We are now using the RPATH method to locate the transition state of such fluorination reactions:

$$(\mathrm{ArI^{+}Ar'Cl^{-}})_2 \rightarrow \mathrm{ArI^{+}Ar'Cl^{-}} \xrightarrow{^{18}\mathrm{F^{-}}} \mathrm{Ar^{18}F/Ar'^{18}F + Ar'I/Ar}$$

Conclusions

The X-ray structure of **1** unveiled hypervalent iodine acting as a stereogenic center. In addition, with the *ab initio* RPATH method, we have identified two additional enantiomers not observed in the crystal structure of **1** as well as two **TS**s for the inversion of the enantiomers. This inversion has the calculated energy barrier of 9.1 kcal/mol in MeCN, and proceeds with an equatorial rotation of the 2-tolyl group with respect to the 2′-anisyl group together with an internal rotation of the 2-tolyl group. Finally, our quantum chemical calculations suggest that **1** likely exists as dimers in MeCN solution because of the strong secondary bonding interaction between the I and Cl atoms of the **M** and **P** forms of **1**. These calculations appear consistent with LC-MS observations of clusters of **1** in weakly organic solution. Taken together, these findings now inform our continuing studies of the radiofluorination of iodonium salts to produce radiotracers for molecular imaging with PET.

Experimental Section

Synthesis of 1

2-Methylphenyl(2′-methoxyphenyl)iodonium chloride (**1)** was synthesized by treating 2-methoxyphenyl boronic acid with 2-[hydroxy(tosyloxy)iodo]toluene[14] followed by anion metathesis of the generated diaryliodonium tosylate with ammonium chloride.

X-Ray crystallography of 1

Crystals of **1** were grown from MeCN solution by portion-wise addition of water at room temperature. X-Ray data were collected using a SMART Apex CCD diffractometer (Bruker, Madison, WI, USA) with graphite-monochromated Mo Kα radiation (λ = 0.71073 Å). Crystal data for **1**: $C_{14}H_{14}ClIO$, M_r = 360.60, triclinic, P-1, T = 100(2) K, a = 7.593(3), b = 9.491(4), c = 10.383(5) Å, V = 697.5(5) Å^3, Z = 2, $\mu(Mo_{Ka})$ = 2.469 mm^{-1}; 5554 reflections

collected, 2764 unique (R_{ini} = 0.0321), GOF = 1.043, final R_1 (I > 2s(I)) = 0.0304, wR_2 = 0.0774. CCDC 710484 (**1**) contains the supplementary crystallographic data for this paper. X-ray structural details (CCDC 710484) can be obtained free of charge from The Cambridge Crystallographic Data Center via www.ccdc.cam.ac.uk/data_request/cif.

Quantum chemistry

To investigate the racemization of **1,** 60 replicas were constructed by combining two sets of 30 replicas in a cyclic pathway. First, 30 replicas were constructed by interpolation between the geometry-minimized **M** and **P** enantiomers of **1,** starting from their X-ray structures, and then another 30 replicas between **P** and **M**. Energy minimization, utilizing CHARMM[15] interfaced with GAMESS[16], was then performed on each replica with an added harmonic penalty function to restrain distances in root-mean square space between adjacent replicas along the reaction pathway in the form

$$E_{rms}=\frac{1}{2}\sum_{i=1}^{N-1}K_{rms}(R_{i,i+1}-<R>)^2 \quad (1)$$

where *N* is the number of replicas i along the pathway; K_{rms} is the force constant (set here to 10^3 kcal/mol/A^2), and $R_{i,i+1}$ and <R> are rmsd values given by

$$R^2_{i,i+1}\sum_{j=1}^{n}w_j=\sum_{j=1}^{n}w_j[(x_j^{(i)}-x_j^{(i+1)})^2+(y_j^{(i)}-y_j^{(i+1)})^2+(z_j^{(i)}-z_j^{(i+1)})^2]$$

$$<R>=N^{-1}\sum_{i=1}^{N-1}R_{i,i+1}$$

where n is the total number of replicated atoms j with coordinates ($x_j^{(k)}$,$y_j^{(k)}$,$z_j^{(k)}$) in replica k, and w_j is a suitable input-defined parameter. Accordingly, the penalty function is proportional to the difference in the rmsd between the two neighboring structures. In addition, an angle energy term Eq. (2), was included to prevent merging between the adjacent points (force constants K_{angle}= 100 and cosmax = 0.95).

$$E_{angle}=\frac{1}{2}\sum_{i=1}^{N-1}K_{angle}((R^2{}_{i,i+2}-R^2{}_{i,i+1}-R^2{}_{i+1,i+2})/(2R_{i,i+1}R_{i+1,i+2})-\cos\max)^2 \quad (2)$$

The average restraint energy shown in Eq. (1) was less than 0.02 kcal/mol per replica after 200 steps of energy minimization. The *ab initio* program GAMESS was used for all RPATH calculations at the B3LYP/DGDZVP level. Further refinement of the approximate TS was carried out with the TS search algorithm using the keywords, opt=(ts, calcfc, noeigentest), as implemented in Gaussian 03 software.[11]

Supplementary Material

Refer to Web version on PubMed Central for supplementary material.

Acknowledgments

This work was supported by the Intramural Research Program of the National Institutes of Health (NIMH and CIT). We are grateful to Dr. S. Hassan (CIT) for discussion, and Dr. M. J. Panzner (University of Akron) for X-ray

analysis of **1**. The quantum chemical study utilized PC/LINUX clusters at the Center for Molecular Modeling of the NIH (http://cit.nih.gov). We are also deeply grateful to Dr. H.U. Shetty (NIMH) for assistance with LC-MS.

References

1. a) Stang PJ, Zhdankin VV. Chem Rev. 1996; 96:1123–1178. [PubMed: 11848783] b) Varvoglis, A. Hypervalent Iodine in Organic Synthesis. Academic Press; London: 1997. c) Varvoglis A, Spyroudis S. Synlett. 1998:221–232. d) Zhdankin VV, Stang PJ. Chem Rev. 2002; 102:2523–2584. [PubMed: 12105935] e) Ochiai M. Top Curr Chem. 2003; 224:5–68. f) Zhdankin VV, Stang PJ. Chem Rev. 2008; 108:5299–5358. [PubMed: 18986207] g) Merritt EA, Olofsson B. Angew Chem Int Ed. 2009; 48:2–21.
2. a) Pike VW, Aigbirhio FI. J Chem Soc, Chem Commun. 1995:2215–2216. b) Gail R, Hocke C, Coenen HH. J Label Compds Radiopharm. 1997; 40:50–52. c) Shah A, Pike VW, Widdowson DA. J Chem Soc, Perkin Trans 1. 1998:2043–2046. c) Martín-Santamaría S, Carroll MA, Carroll CM, Carter CD, Pike VW, Rzepa HS, Widdowson DA. Chem Commun. 2000:649–650. d) Ross TL, Emert J, Hocke C, Coenen HH. J Am Chem Soc. 2007; 129:8018–8025. [PubMed: 17536798] e) Zhang MR, Kumata K, Suzuki K. Tetrahedron Lett. 2007; 48:8632–8635. f) Carroll MA, Nairne J, Smith G, Widdowson DA. J Fluorine Chem. 2007; 128:127–132. g) Cai L, Lu SY, Pike VW. Eur J Org Chem. 2008; 17:2853–2873. h) Telu S, Chun J, Siméon FG, Lu S, Pike VW. J Label Compds Radiopharm. 2009; 52(Suppl 1):S4.
3. a) Beringer FM, Mausner M. J Am Chem Soc. 1958; 80:4535–4536. b) Yamada Y, Kashima K, Okawara M. Polym Lett Ed. 1976; 14:65–71.
4. a) Hacker NP, Leff DV, Dektar JL. J Org Chem. 1991; 56:2280–2282. b) Martín-Santamaría S, Carroll MA, Pike VW, Rzepa HS, Widdowson DA. J Chem Soc, Perkin Trans 2. 2000:2158–2161.
5. a) Alcock NW, Countryman RM. J Chem Soc, Dalton Trans. 1977:217–219. b) Alcock NW, Countryman RM. J Chem Soc, Dalton Trans. 1987:193–196. c) Li H, Jiang S. Acta Cryst. 2007; E63:o83–085. d) Liu CY, Li H, Meng AG. Acta Cryst. 2007; E63:o3647.
6. Woodcock HL, Hodošček M, Sherwood P, Lee YS, Schaefer HF III, Brooks BR. Theor Chem Acc. 2003; 109:140–148.
7. Lee YS, Pike VW, Hodošček M. J Phys Chem A. 2008; 112:1604–1611. [PubMed: 18229901]
8. Miller EG, Rayner DR, Thomas HT, Mislow K. J Am Chem Soc. 1968; 90:4861–4868.
9. a) Archer EM, Van Schalkwyk TGD. Acta Cryst. 1953; 6:88–92. b) Carey JV, Chaloner PA, Hitchcock PB, Neugebauer T, Seddon KR. J Chem Res. 1996; 348:358–359.
10. a) Alcock NW. Adv Inorg Chem. 1972; 15:1–58. b) Landrum GA, Goldberg N, Hoffman R, Minyaev RM. New J Chem. 1998; 22:883–890.
11. Frisch, MJ.; Trucks, GW.; Schlegel, HB.; Scuseria, GE.; Robb, MA.; Cheeseman, JR.; Montgomery, JA., Jr; Vreven, T.; Kudin, KN.; Burant, JC.; Millam, JM.; Iyengar, SS.; Tomasi, J.; Barone, V.; Mennucci, B.; Cossi, M.; Scalmani, G.; Rega, N.; Petersson, GA.; Nakatsuji, H.; Hada, M.; Ehara, M.; Toyota, K.; Fukuda, R.; Hasegawa, J.; Ishida, M.; Nakajima, T.; Honda, Y.; Kitao, O.; Nakai, H.; Klene, M.; Li, X.; Knox, JE.; Hratchian, HP.; Cross, JB.; Adamo, C.; Jaramillo, J.; Gomperts, R.; Stratmann, RE.; Yazyev, O.; Austin, AJ.; Cammi, R.; Pomelli, C.; Ochterski, JW.; Ayala, PY.; Morokuma, K.; Voth, GA.; Salvador, P.; Dannenberg, JJ.; Zakrzewski, VG.; Dapprich, S.; Daniels, AD.; Strain, MC.; Farkas, O.; Malick, DK.; Rabuck, AD.; Raghavachari, K.; Foresman, JB.; Ortiz, JV.; Cui, Q.; Baboul, AG.; Clifford, S.; Cioslowski, J.; Stefanov, BB.; Liu, G.; Liashenko, A.; Piskorz, P.; Komaromi, I.; Martin, RL.; Fox, DJ.; Keith, T.; Al-Laham, MA.; Peng, CY.; Nanayakkara, A.; Challacombe, M.; Gill, PMW.; Johnson, B.; Chen, W.; Wong, MW.; Gonzalez, C.; Pople, JA. Gaussian 03, Revision D.01. Gaussian, Inc; Wallingford CT: 2004.
12. Yu YB, Privalov PL, Hodges RS. Biophys J. 2001; 81:1632–1642. [PubMed: 11509376]
13. Chun JH, Lu SY, Lee YS, Pike VW. J Org Chem. In press.
14. Carroll MA, Pike VW, Widdowson DA. Tetrahedron Lett. 2000; 41:5393–5396.
15. Eurenius KP, Chatfield DC, Hodošček M, Brooks RR. Int J Quantum Chem. 1996; 60:1189–1200.
16. Schmidt MW, Baldridge KK, Boatz JA, Elbert ST, Gordon MS, Jensen JH, Koseki S, Matsunaga N, Nguyen KA, Su S, Windus TL, Dupuis M, Montgomery JA. J Comput Chem. 1993; 14:1347–1363.

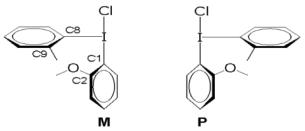

Figure 1.
M and **P** are conformational enantiomers of **1** and are defined, respectively, for the negative and positive Cl–I–C8–C9 (φ_1) dihedral angle.

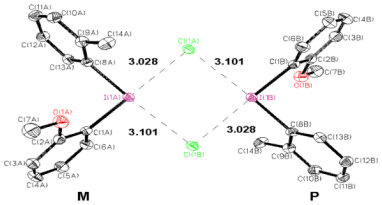

Figure 2.
X-ray crystal structure of dimeric **1** represented in an ORTEP drawing (50% thermal ellipsoids with hydrogen atoms omitted for clarity). Bold numbers are bond distances (Å). Atoms labeled with A and B belong to the **M** and **P** monomers, respectively.

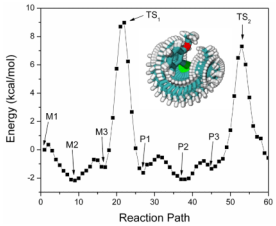

Figure 3.

Potential energy surface for the inversion of **1** in the gas phase from the RPATH calculation having 60 replicas. Energy at each point, without zero point vibration and thermal contribution, is relative to **M1**. Arrows indicate the approximate states. Inset: graphical representation of the 60 replicas. Individual structures are superimposed with the best fit using the six atoms (C1–C6) of the anisyl group of **M1** as the common docking point.

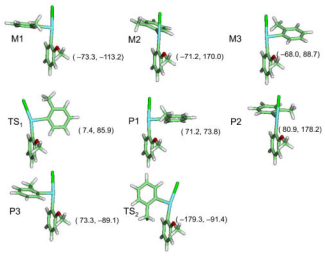

Figure 4.

Conformers of **M** and **P**, and of the two **TS**s. Values in parenthesis indicate the torsional angles, Cl–I–C8–C9 (φ_1) and C8–I–C1–C2 (φ_2); see Figure 1 for atom numbering.

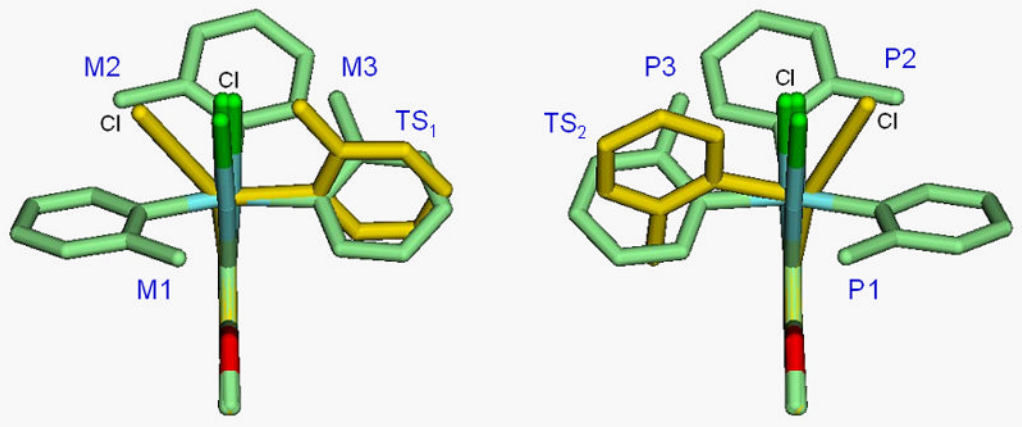

Figure 5.

Overlay of the fully geometry-optimized **M** and **P** conformers (green) and transition states (yellow), using the six atoms (C1–C6) of the anisyl group of **M1** as common docking point. The rmsd of each fit to **M1** is less than 0.07 Å. Each of the pairs of **M1**–**P1**, **M2**–**P2** and **M3**–**P3** is enantiomeric. The Cl atoms of $\mathbf{TS_1}$ and $\mathbf{TS_2}$ d° not align with those of **M** or **P** due to steric repulsion with the tolyl group. Hydrogen atoms are not shown.

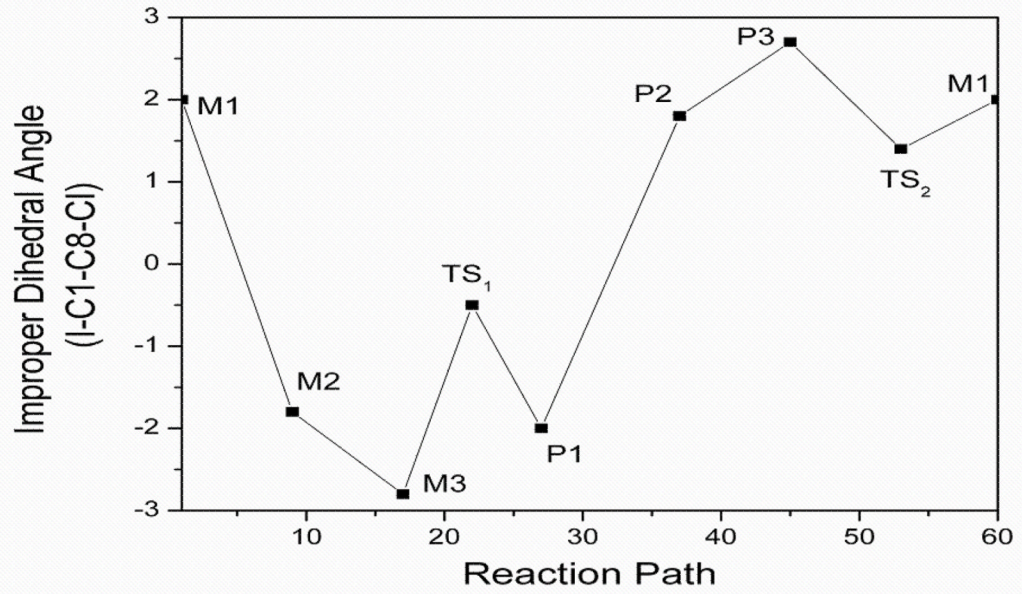

Figure 6.

The variation of the improper dihedral angle of I–C1–C8–Cl along the reaction path shows the inversion of the iodine atom during racemization; the central iodine atom of the **M1** and **P1** pair is located above (2.0°) and below (−2.0°) the plane of C1–C8–Cl, respectively.

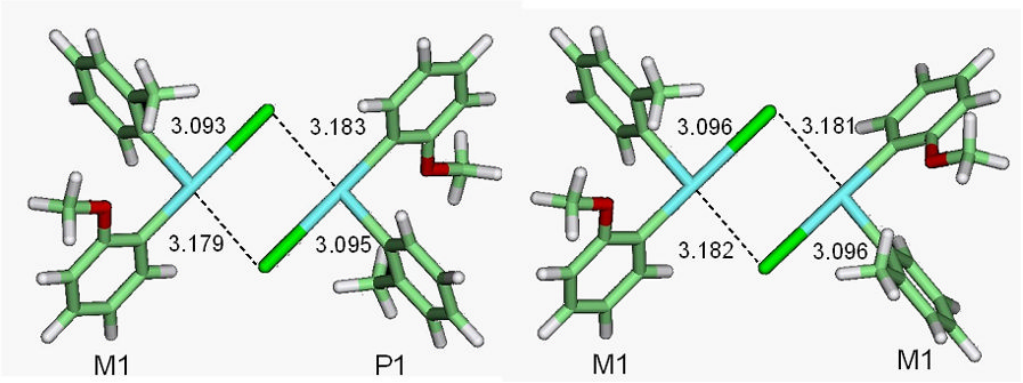

Figure 7.

Geometry-optimized dimers **M1-P1** and **M1-M1** of **1** in MeCN. In **M1-P1**, the 2-methyl and 2′-methoxy groups of **M1** are pointing out of the plane while those of **P1** are pointing into the plane. In the **M1-M1** dimer, all substituents are pointing out of the plane.

Table 1

Calculated energies and geometrical parameters of the conformers and **TS**s of **1** shown in Figure 4 in MeCN at the level of B3LYP/DGDZVP.

Structure	Energy[a] relative to M1 (kcal/mol)	φ_1 Cl–I–C8–C9 (°)	φ_2 C8–I–C1–C2 (°)	I–Cl (Å)
M1	0	− 70.9	− 73.2	2.87
M2	− 0.7	− 77.2	173.6	2.87
M3	− 0.05	− 76.3	82.4	2.86
TS_1	9.1 (− 36.6 cm^{-1})[b]	− 2.6	87.2	3.08
P1	0	71.0	73.3	2.87
P2	− 0.8	77.4	−173.7	2.87
P3	− 0.03	76.1	− 82.6	2.86
TS_2	9.1 (− 39.4 cm^{-1})[b]	179.2	− 88.0	3.01

[a] Energies include the zero-point correction as well as the enthalpy and the entropy contribution at 298.15 K.

[b] Imaginary torsional vibrational mode of the tolyl group.